Spatially-controlled growth of platinum on gold nanorods with tailoring plasmonic and catalytic properties†

Yun Rong,‡[a] Anirban Dandapat,‡[b] Youju Huang,*[a] Yoel Sasson,[b] Lei Zhang,[a] Liwei Dai,[a] Jiawei Zhang,[a] Zhiyong Guo[c] and Tao Chen*[a]

We describe the synthesis of bimetallic dendritic platinum decorated gold nanorods (AuNRs) by the spatial control of Pt growth over gold nanorods using a heterogeneous seed-mediated growth method. The amounts of the Au seed and Pt-precursor were changed to achieve a tunable volume fraction of Pt coverage on the Au NRs surface. Pt nanostructures were spatially separated from each other, which was highly favorable for promising optical and catalytic properties. The dendritic-Pt decorated AuNRs with variable Au/Pt ratios were exploited to study their surface plasmonic properties and catalytic activities. Interestingly, the Pt decorated AuNRs showed strong surface plasmon resonance (SPR) peak due to noncompact dendritic Pt shell in contrast to the conventional core–shell Au@Pt nanoparticles (NPs). Moreover, the longitudinal peak of the AuNRs was finely tuned from 820 to 950 nm (NIR region) by controlling the volume fraction of the Pt decoration over the AuNRs. The catalytic activity of the dendritic-Pt decorated AuNRs on the reduction of 4-nitrophenol (4-NP) by sodium borohydride ($NaBH_4$) as reducing agent was studied and found to be superior to the activities compared to the monometallic Au NRs. Considering practical applications, dendritic-Pt decorated AuNRs nanostructures were immobilized successfully on the hydrophilic polyvinylidene difluoride (PVDF) film as an efficient reusable catalyst.

Introduction

Emerging research has focused on noble metal-based nanostructures to be applied as high-performance catalysts in fields ranging from chemical synthesis and energy conversion to environmental issues. It has been established that bimetallic nanocatalysts often display enhanced physical and chemical properties compared to their monometallic counterparts, as they provide more opportunities to optimize their activity by adjusting the charge transfer between the different metals, local coordination environment, and surface elemental distribution.[1–11] Among the different metal compositions, Au- and Pd-containing bimetallic systems have been extensively studied.[4,7,12] In particular, Pt based catalysts have proven to be most efficient catalyst in various reactions.[10,13–16] Therefore, considering very high cost of Pt, the fabrication of Pt-based catalysts with high performance and as economically as possible is very urgent.

To this end, various Pt-based nanostructures have been synthesized and bimetallic nanostructures were found to be very active compared to only Pt nanoparticles (NPs) as a catalyst.[14,17] Combining another metal (*e.g.*, Ag,[18] Pd,[19,20] Au,[10,21] Fe,[22] and Cu[23]) with Pt not only obtains the benefit of improved bimetallic properties to enhance the catalytic performance, but also reduce the level of the Pt loading to make the materials cheaper. In this direction, we aimed to combine the fascinating properties of Au nanorods (AuNRs),[24–27] such as its unique optical properties, excellent chemical and thermal stability, with the high catalytic activity of tiny Pt NPs.[28–31] However, most reported Au–Pt bimetallic NPs were either alloyed[32] or core–shell structure,[33] and these alloyed or core–shell structure would dramatically inhibit plasmonic property of the Au–Pt bimetallic NPs.[34–37] Herein, we report an effective route to obtain Pt NP decorated Au NRs by the spatial control of Pt growth over Au NRs. By controlling the amounts of the AuNRs and the Pt-precursor, tunable volume fractions of AuNRs were decorated by Pt nanostructures to exploit their structure and composition-dependent optical and catalytic properties. Interestingly, we observed strong surface plasmon resonance peak of the

[a]*Division of Polymer and Composite Materials, Ningbo Institute of Material Technology and Engineering, Chinese Academy of Sciences, No. 1219 Zhongguan West Road, Zhenhai District, Ningbo 315201, China. E-mail: yjhuang@nimte.ac.cn; tao.chen@nimte.ac.cn*

[b]*Casali Center of Applied Chemistry, Institute of Chemistry, The Hebrew University of Jerusalem, Jerusalem 91904, Israel*

[c]*School of Materials Science and Chemical Engineering, Ningbo University, Ningbo 315211, PR China*

dendritic-Pt decorated AuNRs, which is in contrast to most previous reports wherein SPR of the Au core was damped due to Pt deposition.[10,34–37] Because the Pt NPs are spatially separated from each other, it is highly favourable for maximizing the Pt surface area to obtain high catalytic activities. We examined their catalytic activities towards 4-nitrophenol (4-NP) reduction and found superior activities compared to monometallic Au NRs. For practical applications, catalyst in thin film form is highly desirable due to their advanced benefits, *e.g.* easy handling and insertion/removal from the reaction medium *etc.*[38,39] In this study, the dendritic-Pt decorated AuNRs were deposited on the hydrophilic polyvinylidene difluoride (PVDF) film. The nanocomposite films showed excellent catalytic performances and reused for several cycles with much less significant deterioration of their original activity.

Experimental

Materials

Hexadecyltrimethylammonium bromide (CTAB, >99.0%) was purchased from Sigma-Aldrich. Sodium citrate ($C_6H_5Na_3O_7 \cdot 2H_2O$, 99.0%), sodium borohydride ($NaBH_4$, 99.0%), silver nitrate ($AgNO_3$, >99.0%), ascorbic acid (AA, 99.7%), hydrochloric acid (HCl, 37 wt% in water), sodium iodide (NaI, 99.0%) were purchased from Sinopharm Chemical (Shanghai, China). Sodium oleate (NaOL, >97.0%) was purchased from TCI. Hydrogen tetrachloroaurate trihydrate ($HAuCl_4 \cdot 3H_2O$, 99.99%), platinum(II) chloride ($PtCl_2$, 99.0%), 4-nitrophenol (4-NP), tris(hydroxymethyl)aminomethane (Tris), 3-hydroxytyramine hydrochloride (dopamine·HCl) was obtained from Aladdin Company in Shanghai. The other reagents and solvents were of analytical reagent grade and used as received from Sinopharm Chemical Reagent.

Synthesis of gold NRs

The gold nanorods was prepared by a previously reported method.[40] The seed solution was prepared by rapidly injecting 0.6 mL of fresh 0.01 M $NaBH_4$ into the mixture of 5 mL of 0.5 mM $HAuCl_4$ and 5 mL of 0.2 M CTAB solution in a 20 mL scintillation vial under vigorous stirring (1200 rpm). Stirring was stopped after 2 min and the seed solution was aged at room temperature for 30 min before use. To prepare the growth solution, 3.5 g of CTAB and 0.617 g of NaOL were dissolved in 125 mL of warm water. 9 mL of 4 mM $AgNO_3$ solution and 125 mL of 1 mM $HAuCl_4$ solution were added when the solution was cooled to 30 °C. After 90 min of stirring (700 rpm), 0.75 mL of HCl (37 wt% in water, 12.1 M) was introduced to adjust the pH. After another 15 min of slow stirring at 400 rpm, 0.625 mL of 0.064 M ascorbic acid (AA) was added and the solution was stirred vigorously for 30 s. Finally, 0.2 mL seed solution was injected into the growth solution. The resulting mixture was stirred for 30 s and left undisturbed at 30 °C for 12 hours for NRs growth. The resulting nanocrystals were washed twice by centrifugation prior to characterization and re-dispersed in water for further use.

Synthesis of dendritic-Pt decorated AuNRs

Pt decorated AuNRs were prepared by a seed-mediated method, which was slightly different from the previous method[41] by changing the amount of seed solution and the reducing agent. In the presence of iodide ions (50 μM), 10 mL of 0.05 M CTAB, 5 mL of re-dispersed Au nanorods, 500 μL of 0.2 mM $AgNO_3$, and 500 μL of 0.1 M ascorbic acid were added to a vial. The mixture was maintained at 70 °C. After 1 hour, 480 μL of 0.1 M HCl and, 110 μL of 2 mM aqueous H_2PtCl_6 solution were added to the mixture, which was then maintained at 70 °C for 4 h. After this reaction, the sample was centrifuged at 7000 rpm and re-dispersed in deionized water. For the other different volume fractions dendritic platinum coated AuNRs, the aqueous H_2PtCl_6 solution added were 55, 220 and 440 μL.

Catalytic reduction of nitrophenol (4-NP)

The catalytic reduction of 4-NP was monitored on a TU-1810 UV-vis spectrophotometer in the range of 200–600 nm at room temperature. An aqueous solution of 20 μL of 10 mM 4-NP solution and 2.5 mL water were added to 0.1 mL of 0.1 M freshly prepared $NaBH_4$ solution. Subsequently, 0.5 mL of nanoparticle solution was added and mixed thoroughly. Each catalytic experiment was performed at least 3 times to ensure reproducibility. To prepare the dendritic-Pt decorated AuNRs loaded reusable composite film, 20 mL of dendritic-Pt decorated AuNRs synthesized with 440 μL aqueous H_2PtCl_6 solution was added to 20 mL aqueous solution, which contained 2 mg mL^{-1} dopamine and 10 mM Tris buffer solution. The PVDF film was then immersed in the solution for 4 days at room temperature. The PVDF membrane was prepared using the previously reported method.[42] The dendritic-Pt decorated AuNRs loaded PVDF film was washed three times with running water and dried in air. For the cyclic catalytic performance of the dendritic-Pt decorated AuNRs loaded PVDF film, the film was cut into a 1 cm × 4 cm piece then immersed into an aqueous solution of 20 μL of 10 mM 4-NP solution, 2.5 mL of water and 0.1 mL of 0.1 M freshly prepared $NaBH_4$ solution for 2 hour. The film was washed three times with running water and dried in air for the next catalytic performance test. The experiment was repeated 7 times.

Characterization

Ultraviolet-visible (UV-vis) absorption spectra were obtained with TU-1810 spectrophotometer from Beijing Purkinje General Instrument Co. Ltd. in transmission mode. Transmission electron microscopy (TEM) was performed on a JEOL JEM-2100F instrument and operated at 200 kV. Scanning electronic microscopy (SEM) was carried out using a JEOL JMS-6700F scanning microscope.

Results and discussion

A heterogeneous seed-mediated growth route was introduced to produce the bimetallic dendritic-Pt decorated AuNRs, as illustrated schematically in Fig. 1a. The nanostructures were characterized by UV-visible spectroscopy and TEM. Au NRs (aspect

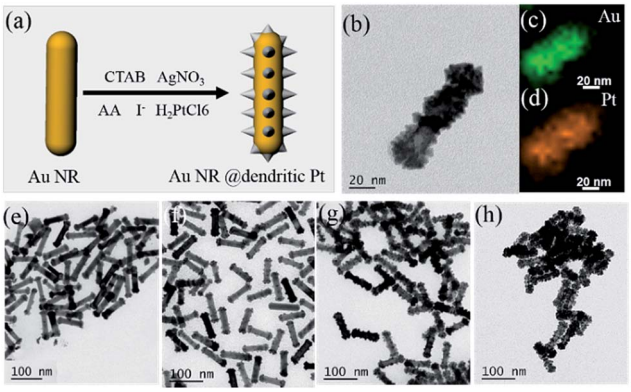

Fig. 1 (a) Scheme of the synthesis of dendritic-Pt decorated AuNRs; (b) TEM images of dendritic-Pt decorated AuNRs. (c) and (d) Show the elemental mappings of one dendritic-Pt decorated AuNRs. The green and orange colours in the elemental maps stand for gold and platinum, respectively; TEM images (e–h) of nanostructures with varying volume fractions dendritic platinum obtained by adding different amounts of a 2 mM H_2PtCl_6 solution: (e) 55 μL, (f) 110 μL, (g) 220 μL and (h) 440 μL, respectively.

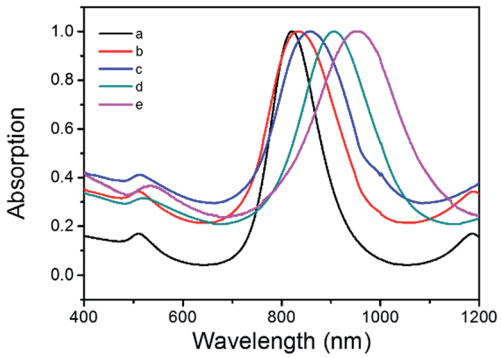

Fig. 2 UV-vis absorption spectra of (a) Au NR and (b–e) Au NR decorated with dendritic platinum synthesized with different amount of 2 mM H_2PtCl_6 solution (55 μL in (b), 110 μL in (c), 220 μL in (d) and 440 μL in (e), respectively).

ratio ~3; Fig. S1†) were first synthesized in an aqueous solution employing a binary mixture of surfactant, namely, CTAB and NaOL.[40] Furthermore, the dendritic-Pt decorated AuNRs were prepared *via* the heterogeneous seed-mediated growth of Pt nanostructures over the Au NR seeds by reducing H_2PtCl_6 with ascorbic acid under the assistance of CTAB, iodide ions and Ag^+ ions. As revealed by HR-TEM (Fig. 1b) and elemental mapping (Fig. 1c and d), the dendritic Pt shell is composed of many small Pt nanostructures with a size of ~4–5 nm. The Pt growth on the Au NRs was controlled spatially to achieve different volume fractions of Pt-nanostructure coverage over the Au NRs (ESI; Fig. S2†) by controlling the amounts of Pt-precursor, *i.e.* H_2PtCl_6 in a fixed amount of Au NRs seed solution. First, Pt nanostructures were selectively deposited at the tips of Au NRs (Fig. 1e & S3a†) in the presence of iodide ions and Ag^+, beacause the surface energy is higher and the co-ordination number is lower at the tips of the AuNRs.[41] A higher surface energy and lower coordination number generates more reactive sites at the tips, and Pt prefers to be deposited on the tips of the NRs.[41] With increasing amounts of H_2PtCl_6 (2 mM) solution from 55 μL to 440 μL, as shown by the TEM images (Fig. 1e–h and S3†), the tips of the Au NRs was first covered with tiny Pt NPs (Fig. 1e) followed by deposition on the side faces, finally forming dendritic discontinuous Pt-shell over the Au NRs (Fig. 1h). Much larger amounts of H_2PtCl_6 solution (5 mL; 2 mM) produced core–shell AuNR@Pt nanostructures (ESI; Fig. S4†). These dendritic-Pt decorated AuNRs were highly monodisperse, as revealed by their TEM (Fig. 1) and SEM (ESI; Fig. S5†) images. Owing to this unique dendritic structure, both Au and Pt surfaces remain highly accessible by the reactants, which will make the nanostructures efficient for catalytic applications.

The optical properties of Au and dendritic-Pt decorated AuNRs were characterized by UV-vis absorption spectroscopy. Fig. 2 shows the UV-vis absorption spectra of the as-prepared Au NRs (a) and the dendritic-Pt decorated AuNRs (b–e). As can be observed from Fig. 2, Au NRs display two characteristic absorption peaks at 515 and 820 nm, corresponding to a weak transverse surface plasmon (TSP) resonance and a strong longitudinal surface plasmon (LSP) resonance, respectively. Interestingly, we observed a gradual red-shift of the longitudinal peak with fine tuning from 820 nm to 950 nm by controlling the amounts of 2 mM H_2PtCl_6 (55 μL to 440 μL), whereas the transverse resonance wavelength was shifted slightly or remained unchanged (ESI; Fig. S6†). The much higher shifting of the longitudinal peak results from the higher polarizability of the NRs at the longitudinal plasmon resonance than at the transverse plasmon resonance.[43] The red-shift can be correlated with the discontinuous dendritic growth of Pt shell similar to the case of the Au@Pd system.[44] In a previous report, Chen *et al.*[44] established that a discontinuous Pd shell on Au NR causes a red-shift, whereas continuous Pd shell showed a blue-shift of the SPR of the Au NR core. In a similar way, we could tune the longitudinal peak of dendritic-Pt decorated AuNRs from 820 nm to 950 nm (NIR region) by controlling the fraction of Pt coverage over the AuNR's surface. This tunable localized surface plasmon resonance wavelength towards the NIR region is very useful for biomedical applications as well as for the *in situ* spectroscopic characterization of some catalytic reactions.

This interesting dendritic morphology of the nanostructures with varying Au/Pt composition ratio motivated us to explore the catalytic activity of the nanostructures. The reduction of 4-NP by $NaBH_4$ in an aqueous solution is a well-known and easily monitored reaction, and was chosen as a model reaction to test the catalytic activities of the developed materials.[45] The reaction was monitored by collecting the UV-visible absorption spectrum of the mixture of 4-NP and $NaBH_4$ at different times. Initially, the solution showed absorption maxima at ~400 nm due to the formation of 4-nitrophenolate ions in alkaline solution, which is caused by the addition of $NaBH_4$ solutions. This absorption spectrum remained almost unaltered with time in the absence of a catalyst, which suggests that the reduction did not proceed. In the contrary, the presence of very small amounts of Au–Pt nanostructures causes the reduction of 4-NP very rapidly as

observed in their time-dependent UV-visible absorption spectra (Fig. 3a).

In addition to the successive decrease in the absorption peak at 400 nm, a new peak at 280 nm developed gradually due to the reduction of 4-NP to 4-aminophenol (4-AP). We performed the catalytic activities of all the different nanostructures and a representative study using dendritic-Pt decorated AuNRs (Fig. 1h; nanostructures synthesized using 440 μL of H_2PtCl_6 solution) as a catalyst is presented in Fig. 3a. The rate constants were calculated by plotting $\ln(C_t/C_0)$ (where C_0 and C_t are the concentrations of 4-AP at time zero and t, respectively) as a function of time for all the structures and have been presented in Fig. 3b and Table S1.† The activity was increased gradually with increasing Pt loading. However, fully covered AuNR@Pt core–shell nanostructures showed lower activity compared to dendritic-Pt decorated AuNRs obtained by adding 440 μL of 2 mM H_2PtCl_6 solution (ESI; Fig. S7†). The result is consistent with a previous report by Zheng *et al.*,[46] wherein an improved catalytic activity was observed by Pd-tipped Au NRs compared to that of the core–shell AuNR@Pd nanostructures towards 4-NP reduction. The enhanced catalytic activities of the Pd-tipped AuNRs were attributed to hot electron transfer from Au to Pd. The interfacial interaction between two different metal segments is essential for the improved catalysis. In a similar way, our developed dendritic-Pt decorated AuNRs with the simultaneous exposure of Pt and Au surfaces result in improved catalytic activity over the core–shell nanostructure.

It is widely accepted that the catalytic reduction of 4-NP by any metal NPs catalyst involved the adsorption of both BH_4^- and 4-NP from aqueous solution on the surface of the NPs, and then electron/hydride transfer from BH_4^- to 4-NP to produce 4-AP.[17,45] It can be noted that 4-NP prefers to adsorb on Au, whereas BH_4^- is more likely to adsorb on Pt.[17] Therefore, the mechanism for the reduction of 4-NP by $NaBH_4$ in presence of the developed bimetallic dendritic-Pt decorated AuNRs could be proposed, as illustrated in Fig. 4. First, 4-nitrophenolate and BH_4^- ions are adsorbed on the neighbouring Au and Pt sites, respectively, at the surface of dendritic-Pt decorated AuNRs. BH_4^- produces transient metal hydrides with Pt atoms and then the adsorbed hydrogens were transferred to 4-nitrophenolate ion adsorbed adjacent Au sites and reduced to 4-AP. Owing to this synergistic effect of Au and Pt, bimetallic dendritic-Pt decorated AuNRs showed better catalytic activity than that of Au NRs.

In a successful catalytic reaction, the reusability of the catalyst is very important. In this study, we developed a composite film, wherein dendritic-Pt decorated AuNRs were deposited on a PVDF film by the mussel inspired polymer polydopamine (PDA). PDA can be deposited easily on virtually all types of inorganic and organic substrates.[47] Recently, PDA has been applied in various catalytic systems and served as a catalyst carrier due to its unique merits.[48] The colour of the PVDF film was changed from white to black-brown (Fig. 5a and b), indicating the successful deposition of dendritic-Pt decorated AuNRs on the PVDF film. To further confirm the deposition of the dendritic-Pt decorated AuNRs on the PVDF film, the morphology of the PVDF film before and after the deposition of dendritic platinum decorated Au NRs were analysed by SEM. The PVDF film has a porous multilayer structure (Fig. 5c) with the unique properties of a high specific surface area and chemical stability, which is an ideal candidate as catalyst carrier. The dendritic-Pt decorated AuNRs were immobilized and randomly dispread on the PVDF film (Fig. 5d).

The catalytic property of this nanocomposite film was tested in seven consecutive cycles (Fig. 6a). After each cycle, the catalyst film was withdrawn directly from the reaction solution, washed with water, and allowed to perform the next cycle. As revealed in Fig. 6b, almost identical catalytic activities were observed. Almost 90% conversion was measured even at the seventh cycle, indicating the excellent stability and recyclability

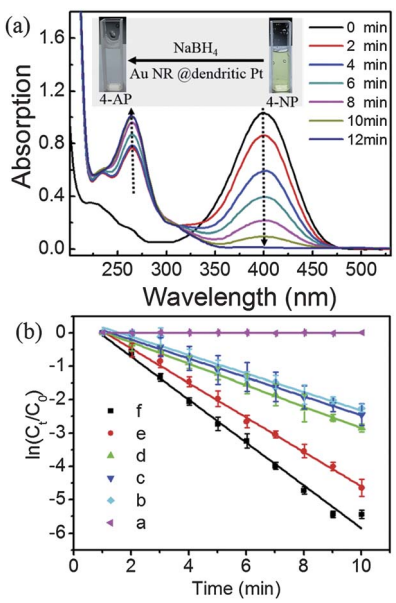

Fig. 3 (a) Time-dependent UV-vis absorption spectra of 4-NP reduced by $NaBH_4$ and catalyzed by dendritic-Pt decorated AuNRs. (b) Plot of $\ln(C_t/C_0)$ as a function of time of different catalyst ((a), no catalyst; (b), AuNR; (c–f), dendritic-Pt decorated AuNRs synthesized with different amounts of 2 mM H_2PtCl_6 solution (55 μL in (c), 110 μL in (d), 220 μL in (e) and 440 μL in (f), respectively)).

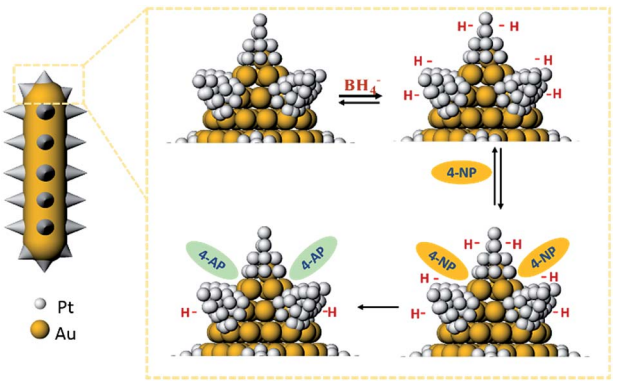

Fig. 4 Schematic for the possible mechanism of 4-NP reduction on dendritic-Pt decorated AuNR's surface.

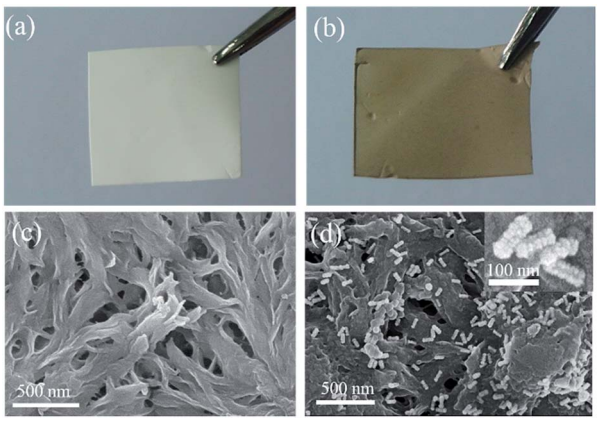

Fig. 5 Digital photos (a and b) and SEM images (c and d) of PVDF film before (a and c) and after (b and d) the deposition of dendritic-Pt decorated AuNRs.

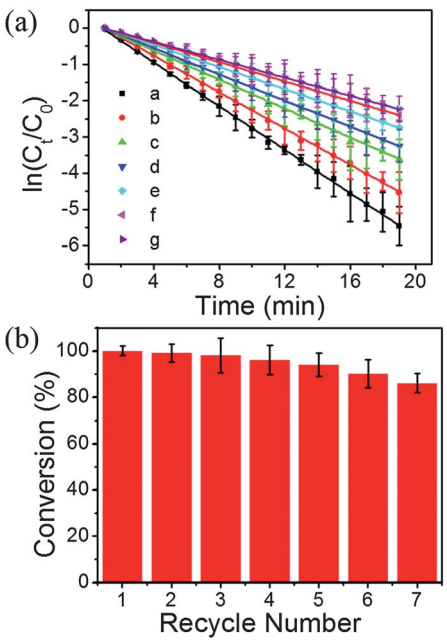

Fig. 6 Plot of $\ln(C_t/C_0)$ as a function of time of 4-NP and (b) conversion efficiency of 4-NP in 2 hours reaction in seven successive cycles using dendritic-Pt decorated AuNRs on the PVDF film as catalyst (a–g represent the recycle 1–7, respectively).

of the catalytic films. The dendritic-Pt decorated AuNRs deposited PVDF film also possessed the property of oil/water separation[42] (oil/water separation result is shown in Fig. S8†), which would provide new opportunities to develop a bifunctional membrane with both catalytic and oil/water separation properties.

Conclusions

We reported the synthesis of dendritic-Pt decorated AuNRs by spatially controlled Pt growth over the Au NRs in a facile wet chemical method and the synthesized hybrid bimetallic nanostructures exhibit tunable localized surface plasmon resonance from the visible to NIR region as well as excellent catalytic activity. We demonstrated that catalysis and optical properties of the hybrid nanostructures can be tailored readily by adjusting the surface decoration density of the Pt NPs on the surfaces of the Au NRs. Pt NPs remained spatially separated from each other, which is favourable for maximizing the Pt surface area to obtain very high catalytic activities. For successful catalytic application, the nanostructures were loaded in a solid PVDF film support and the composite film was used as an efficient catalyst, maintaining excellent stability and reusability. Apart from the catalytic activities, considering their very interesting optical properties, these unique materials need to be applied in various biomedical applications.

Acknowledgements

We thank the Chinese Academy of Science for Hundred Talents Program, Chinese Central Government for Thousand Young Talents Program, the Natural Science Foundation of China (21404110, 51473179, 81273130 and 51573203), the Ningbo Science and Technology Bureau (Grant 2014B82010 and 2015C110031), the Technology Foundation for Selected Overseas Chinese Scholar, and Ministry of Personnel of China (2015).

References

1 X. Peng, Q. Pan and G. L. Rempel, *Chem. Soc. Rev.*, 2008, **37**, 1619–1628.
2 M. T. Reetz, M. Winter, G. Dumpich, J. Lohau and S. Friedrichowski, *J. Am. Chem. Soc.*, 1997, **119**, 4539–4540.
3 L. Zhu, L. Zheng, K. Du, H. Fu, Y. Li, G. You and B. H. Chen, *RSC Adv.*, 2013, **3**, 713–719.
4 D. Jana, A. Dandapat and G. De, *J. Phys. Chem. C*, 2009, **113**, 9101–9107.
5 N. Sharma, H. Ojha, A. Bharadwaj, D. P. Pathak and R. K. Sharma, *RSC Adv.*, 2015, **5**, 53381–53403.
6 L. Kuai, X. Yu, S. Wang, Y. Sang and B. Geng, *Langmuir*, 2012, **28**, 7168–7173.
7 R. Su, R. Tiruvalam, A. J. Logsdail, Q. He, C. A. Downing, M. T. Jensen, N. Dimitratos, L. Kesavan, P. P. Wells, R. Bechstein, H. H. Jensen, S. Wendt, C. R. A. Catlow, C. J. Kiely, G. J. Hutchings and F. Besenbacher, *ACS Nano*, 2014, **8**, 3490–3497.
8 A. Mattiuzzi, I. Jabin, C. Mangeney, C. Roux, O. Reinaud, L. Santos, J.-F. Bergamini, P. Hapiot and C. Lagrost, *Nat. Commun.*, 2012, **3**, 1130.
9 S. Guo, J. Li, S. Dong and E. Wang, *J. Phys. Chem. C*, 2010, **114**, 15337–15342.
10 H. Ataee-Esfahani, L. Wang, Y. Nemoto and Y. Yamauchi, *Chem. Mater.*, 2010, **22**, 6310–6318.
11 Y. Huang, P. Kannan, L. Zhang, T. Chen and D.-H. Kim, *RSC Adv.*, 2015, **5**, 58478–58484.
12 O. V. Belousov, N. V. Belousova, A. V. Sirotina, L. A. Solovyov, A. M. Zhyzhaev, S. M. Zharkov and Y. L. Mikhlin, *Langmuir*, 2011, **27**, 11697–11703.

13 T.-D. P.-o.-A. Bimetallic, *J. Phys. Chem. C*, 2010, **114**, 15337–15342.
14 B. Lim, M. Jiang, P. H. C. Camargo, E. C. Cho, J. Tao, X. Lu, Y. Zhu and Y. Xia, *Science*, 2009, **324**, 1302–1305.
15 C. Q. Wang, F. F. Ren, C. Y. Zhai, K. Zhang, B. B. Yang, D. A. Bin, H. W. Wang, P. Yang and Y. K. Du, *RSC Adv.*, 2014, **4**, 57600–57607.
16 Y.-W. Lee, A. R. Ko, D.-Y. Kim, S.-B. Han and K.-W. Park, *RSC Adv.*, 2012, **2**, 1119–1125.
17 C. Chu and Z. Su, *Langmuir*, 2014, **30**, 15345–15350.
18 Y. Huang, P. Kannan, L. Zhang, Y. Rong, L. Dai, R. Huang and T. Chen, *RSC Adv.*, 2015, **5**, 94849–94854.
19 Y. Huang, A. R. Ferhan, A. Dandapat, C. S. Yoon, J. E. Song, E. C. Cho and D.-H. Kim, *J. Phys. Chem. C*, 2015, **119**, 26164–26170.
20 J. Zhang, Y. Mo, M. B. Vukmirovic, R. Klie, K. Sasaki and R. R. Adzic, *J. Phys. Chem. B*, 2004, **108**, 10955–10964.
21 Y. Jin and S. Dong, *J. Phys. Chem. B*, 2003, **107**, 12902–12905.
22 S. Guo and S. Sun, *J. Am. Chem. Soc.*, 2012, **134**, 2492–2495.
23 S. Zhou, B. Varughese, B. Eichhorn, G. Jackson and K. McIlwrath, *Angew. Chem., Int. Ed.*, 2005, **117**, 4615–4619.
24 Y. Huang, A. R. Ferhan and D.-H. Kim, *Nanoscale*, 2013, **5**, 7772–7775.
25 Y. Huang and D.-H. Kim, *Nanoscale*, 2011, **3**, 3228–3232.
26 Y. Huang, L. Wu, X. Chen, P. Bai and D.-H. Kim, *Chem. Mater.*, 2013, **25**, 2470–2475.
27 T. Xie, C. Jing, W. Ma, Z. Ding, A. J. Gross and Y.-T. Long, *Nanoscale*, 2015, **7**, 511–517.
28 A. Dandapat, D. Jana and G. De, *ACS Appl. Mater. Interfaces*, 2009, **1**, 833–840.
29 B. Sheng, L. Hu, T. Yu, X. Cao and H. Gu, *RSC Adv.*, 2012, **2**, 5520–5523.
30 C. Zhang, Y. Zhou, Y. Zhang, Q. Wang and Y. Xu, *RSC Adv.*, 2015, **5**, 12472–12479.
31 A. Dandapat, A. Mitra, P. K. Gautam and G. De, *Nanomater. Nanotechnol.*, 2013, **3**, 11.
32 Y.-C. Lu, Z. Xu, H. A. Gasteiger, S. Chen, K. Hamad-Schifferli and Y. Shao-Horn, *J. Am. Chem. Soc.*, 2010, **132**, 12170–12171.
33 K.-J. Chen, W.-N. Su, C.-J. Pan, S.-Y. Cheng, J. Rick, S.-H. Wang, C.-C. Liu, C.-C. Chang, Y.-W. Yang and C.-H. Wang, *J. Mater. Chem. B*, 2013, **1**, 5925–5932.
34 G. De and C. N. R. Rao, *J. Mater. Chem. C*, 2005, **15**, 891–894.
35 H.-D. Koh, S. Park and T. P. Russell, *ACS Nano*, 2010, **4**, 1124–1130.
36 M. Cheng, M. Zhu, Y. Du and P. Yang, *Int. J. Hydrogen Energy*, 2013, **38**, 8631–8638.
37 Z. Y. Bao, D. Y. Lei, R. Jiang, X. Liu, J. Dai, J. Wang, H. L. W. Chan and Y. H. Tsang, *Nanoscale*, 2014, **6**, 9063–9070.
38 A. Dandapat and G. De, *J. Mater. Chem.*, 2010, **20**, 3890–3894.
39 H. Gnayem, A. Dandapat and Y. Sasson, *Chem.–Eur. J.*, 2016, **22**, 370–375.
40 X. Ye, C. Zheng, J. Chen, Y. Gao and C. B. Murray, *Nano Lett.*, 2013, **13**, 765–771.
41 S. Ham, H. J. Jang, Y. Song, K. L. Shuford and S. Park, *Angew. Chem.*, 2015, **127**, 9153–9156.
42 M. Tao, L. Xue, F. Liu and L. Jiang, *Adv. Mater.*, 2014, **26**, 2943–2948.
43 H. Chen, L. Shao, Q. Li and J. Wang, *Chem. Soc. Rev.*, 2013, **42**, 2679–2724.
44 H. Chen, F. Wang, K. Li, K. C. Woo, J. Wang, Q. Li, L.-D. Sun, X. Zhang, H.-Q. Lin and C.-H. Yan, *ACS Nano*, 2012, **6**, 7162–7171.
45 S. Wunder, F. Polzer, Y. Lu, Y. Mei and M. Ballauff, *J. Phys. Chem. C*, 2010, **114**, 8814–8820.
46 Z. Zheng, T. Tachikawa and T. Majima, *J. Am. Chem. Soc.*, 2015, **137**, 948–957.
47 Y. Liu, K. Ai and L. Lu, *Chem. Rev.*, 2014, **114**, 5057–5115.
48 A. Ma, Y. Xie, J. Xu, H. Zeng and H. Xu, *Chem. Commun.*, 2015, **51**, 1469–1471.